Electronic Supplementary Material (ESI) for Nanoscale.

Supporting information for

Non-invasive monitoring of biochemicals in hydrogel assisted microfluidic chips

Na Zhao,[1] Zehua Yu,[1] Jun Huang,[1 *] Yuxi Liu,[1] Yifan Zhao,[1] Xiangqian Fu[1 *] Peihua Yang,[2] and Kang Liu[1 *]

[1] MOE Key Laboratory of Hydraulic Machinery Transients, School of Power and Mechanical Engineering, Wuhan University, Wuhan 430072, China

[2] The Institute of Technological Sciences, Wuhan University, Wuhan 430072, China

[*] huangjunkimi@whu.edu.cn; fmlab@whu.edu.cn; kang.liu@whu.edu.cn

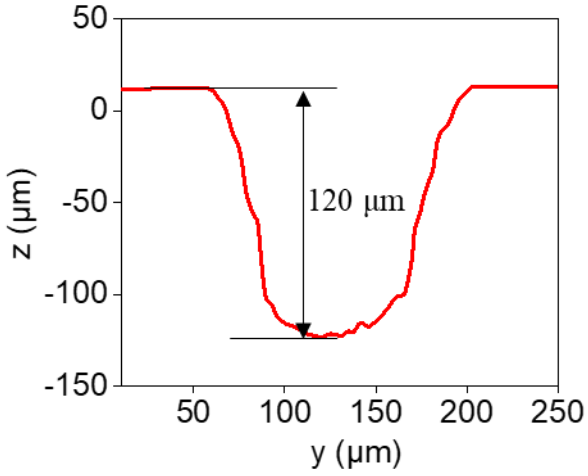

Figure S1. Height profile of the microchannel measured by the optical profilometer.

Figure S2. Fabrication process of the hydrogel microfluidic chip.

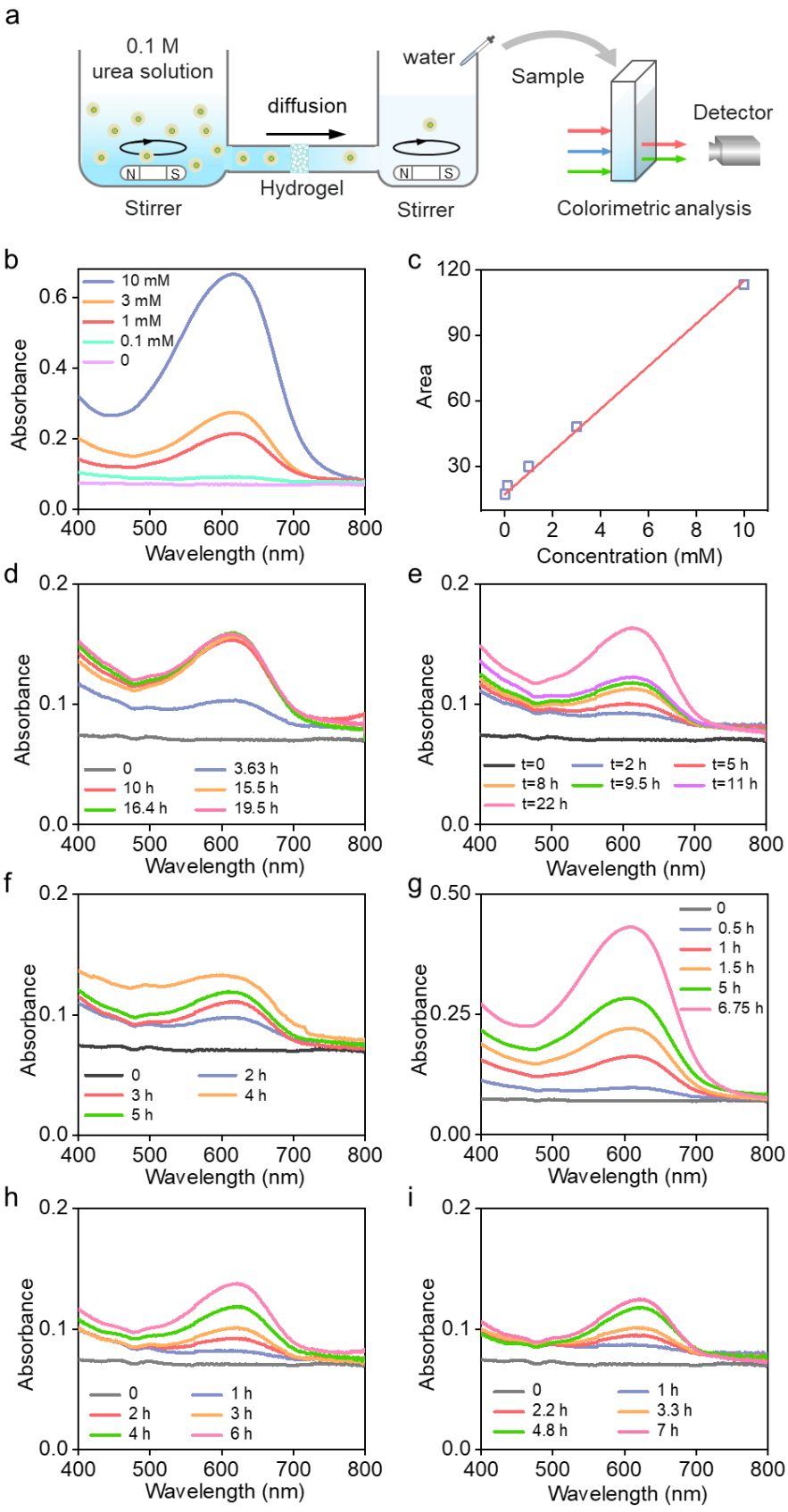
a
0.1 M
urea solution
diffusion
water
Sample
Detector
Hydrogel
Stirrer
Stirrer
Colorimetric analysis
b
10 mM
3 mM
1 mM
0.1 mM
0
Absorbance
Wavelength (nm)
c
Area
Concentration (mM)
d
0
3.63 h
10 h
15.5 h
16.4 h
19.5 h
Absorbance
Wavelength (nm)
e
t=0
t=2 h
t=5 h
t=8 h
t=9.5 h
t=11 h
t=22 h
Absorbance
Wavelength (nm)
f
0
2 h
3 h
4 h
5 h
Absorbance
Wavelength (nm)
g
0
0.5 h
1 h
1.5 h
5 h
6.75 h
Absorbance
Wavelength (nm)
h
0
1 h
2 h
3 h
4 h
6 h
Absorbance
Wavelength (nm)
i
0
1 h
2.2 h
3.3 h
4.8 h
7 h
Absorbance
Wavelength (nm)

Figure S3. Measurement of urea diffusivity. (a) Schematic of the measurement system. (b) Calibration of the absorption spectroscopy of the blue indophenol produced from the urease hydrolysis reaction. (c) The relationship between the peak area of 600 nm absorption band and urea concentration; time evolution of the absorption spectroscopy measured from (d) pHEMA-6%, (e) pHEMA-2%, (f) pAAm, (g) pAAc, (h) pAA-SA and (i) pDMAPS.

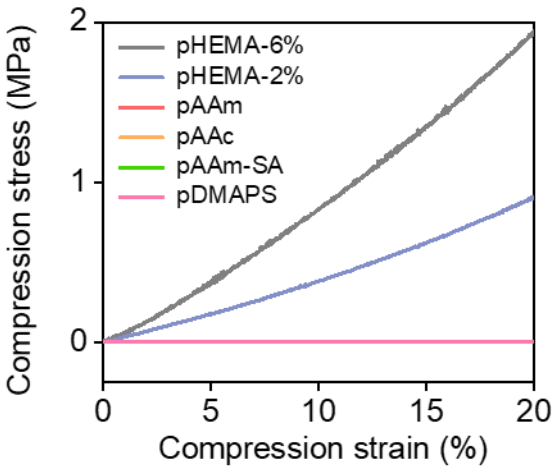

Figure S4. Compressive stress strain curve of tested hydrogel. Samples were prepared as blocks by a 10 mm × 10 mm × 7 mm mold.

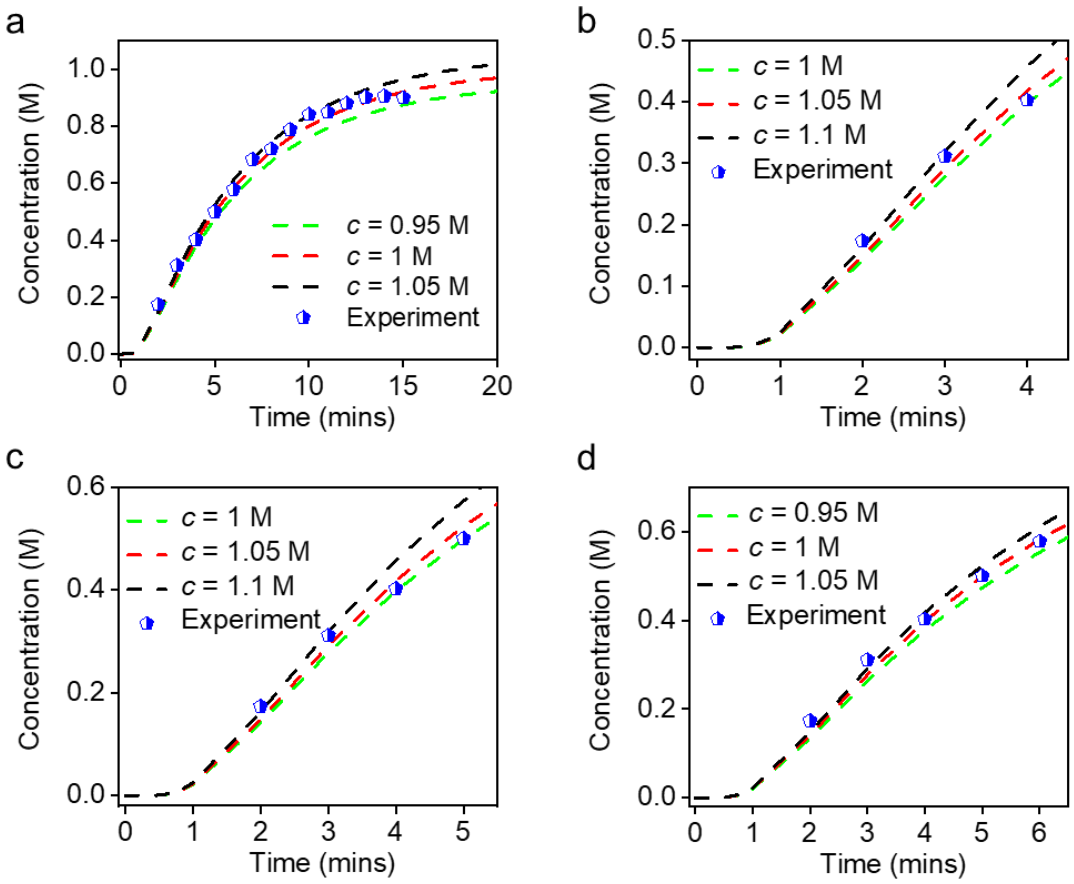

Figure S5. Experiment and theoretical concentration variation with time at the hydrogel surface. Blue pentagons are the experimental data. Lines are the fitting curves. The figures show the theoretical fitting with experimental results within (a) 15 minutes, (b) 4 minutes, (c) 5 minutes, and (d) 6 minutes.

The microfluidic flow in the micro-channel is governed by Navier-Stokes equations. The viscous flow through porous media is governed by Brinkman equation:[1]

$$\mu\nabla^2\mathbf{u} - \nabla p - \mu\alpha^2\mathbf{u} = 0 \tag{1a}$$

$$\nabla\bullet\mathbf{u} = 0 \tag{1b}$$

where μ is the viscosity, α is the permeability, and **u** and p are the average velocity and pressure, respectively. The transport of urea molecules in the hydrogel sealing window was depicted by derivation of Fick's second low:

$$\frac{\partial c_i}{\partial t} = D_i \nabla^2 c_i \tag{2}$$

where c is the concentration of urea, D is the diffusion coefficient. The flow rate at the inlet boundary was 80 μL min^{-1}. The outlet was set as an open boundary condition. The bottom boundary was treated as an axisymmetric boundary. Other boundaries except the interface between micro-channel and hydrogel was considered as wall. The initial condition was set as,

$$\mathbf{u} = \mathbf{u}_0 \tag{3a}$$

$$c = c_0 \tag{3b}$$

where $\mathbf{u}_0$ is the inlet velocity, and c_0 is the inlet concentration.

The critical parameter of urea diffusivity was set as a position-varying value due to the water content different along thickness direction. At the solution/hydrogel interface, the pHEMA is fully hydrated. While at the surface of the hydrogel, the pHEMA is partially dehydrated. Within the hydrogel, the water content and the porosity are linearly varied, and the water content is measured to be linearly varied along the thickness direction. Besides, the diffusivity is linearly correlated with the porosity. Thus, the diffusivity of urea (D_{urea}) changes linearly with through-thickness position (z), D_{urea}=-1.857×10^{-8}·z+2.933×10^{-9}. z=0 represents for the position of the microfluid/hydrogel interface. The diffusivity of water was taken as 5.5×10^{-6} $cm^2 \cdot s^{-1}$.[2]

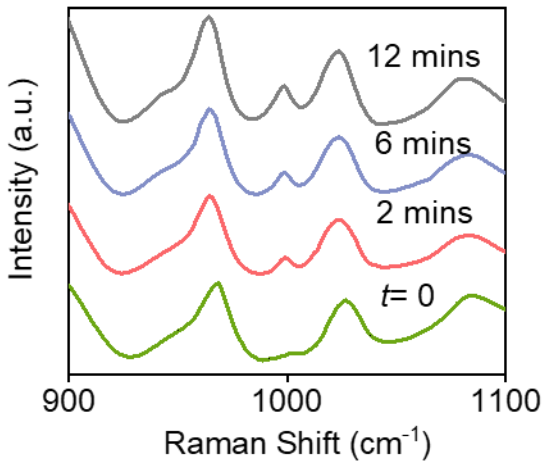

Figure S6. Time evolution of the Raman spectroscopy measured from the pHEMA microfluidic chip.

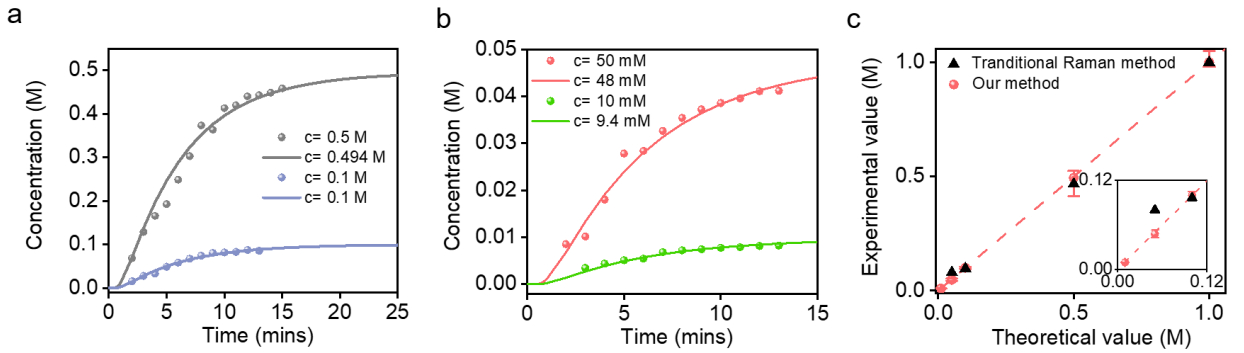

Figure S7. Measurement results of the pHEMA-assisted non-invasive microfluidic chip under different urea concentrations. (a) Measurement results of 0.5 mol L^{-1} and 0.1 mol L^{-1}. (b) Measurement results of 50 mmol L^{-1} and 10 mmol L^{-1}. Spheres are experiment results. Lines are fitting curves obtained from numerical solution. (c) Comparison of experimental measured values and theoretical values of the microfluidic concentration. Red spheres represent measurement results obtained from our method. Black triangles represent results obtained from traditional Raman method through a PDMS window. The red dashed line represents that the experimental result equals to the theoretical value. Inset figure is an enlarged view in low concentration region.

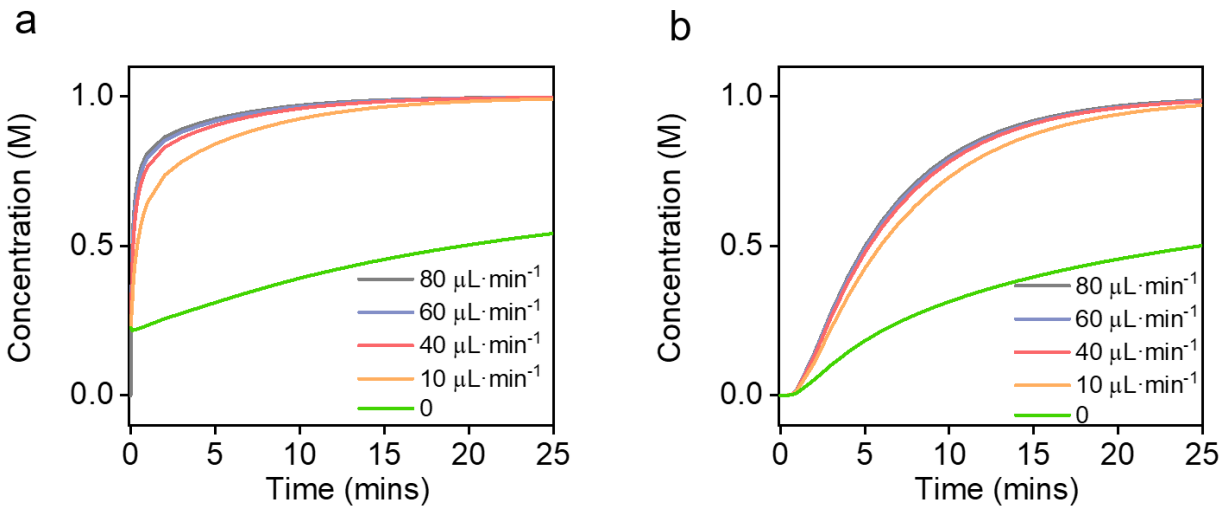

Figure S8. Variation of urea concentration with time at the (a) bottom surface and (b) the upper surface of the hydrogel under different flow rates in the microchannel.

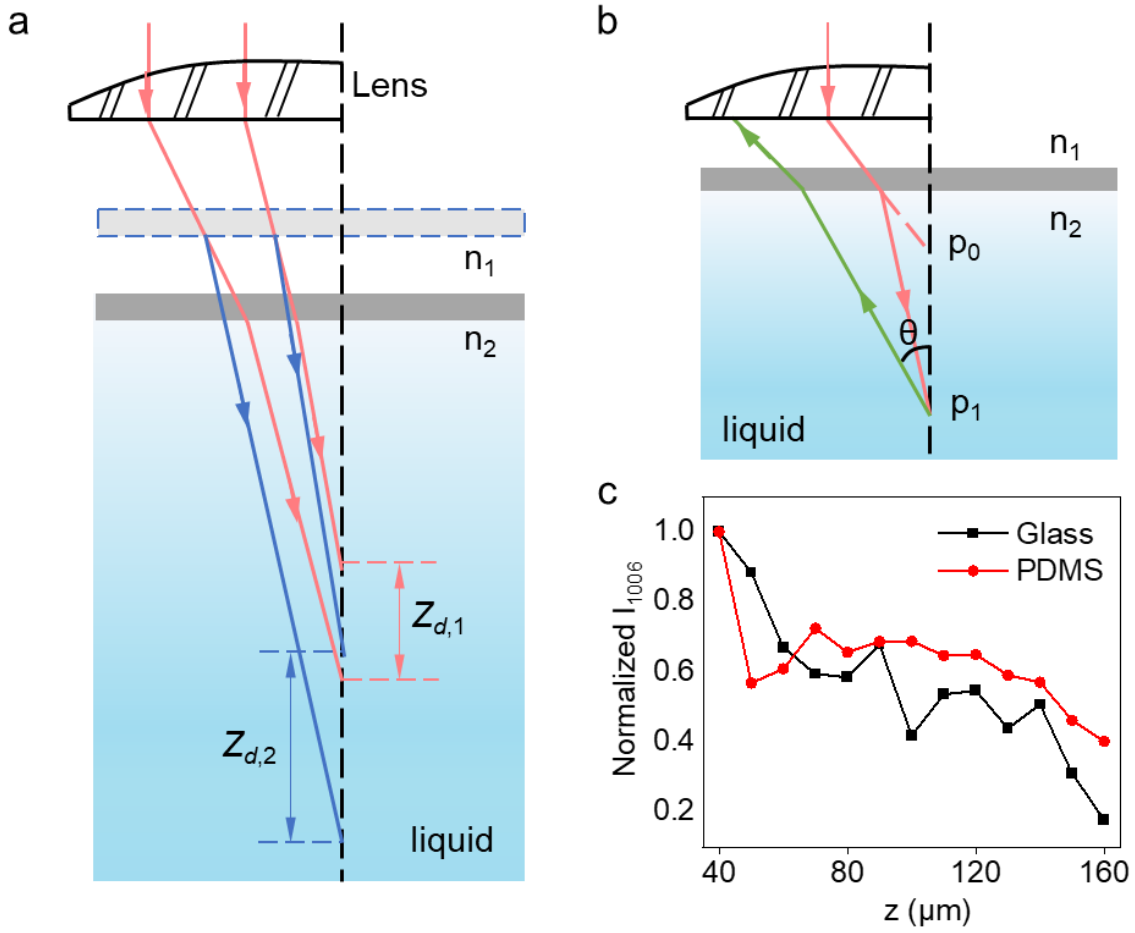

Figure S9. The effect of refraction through a planar interface on the depth of focus and collection efficiency. (a) Schematic of the effect of refraction with different focusing depth in the channel. (b) The interface-induced aberrations on the confocal collection of the Raman scattered light. (c) The measured Raman intensity variation with the focusing depth through a glass or PDMS window with the urea concentration of 50 mM in the channel.

As shown in Figure S9(a), the laser comes from the edge of the objective lens is focused at a deeper position than that comes from the central part of the lens. The distance between these points is defined as the depth resolution (z_d). As the focus depth increases (from red line indicated position to blue one), the depth resolution gets worse. The depth resolution can be quantitatively obtained from the numerical aperture of the objective (NA), the refractive index of the medium (n), and the ideal focus depth (d_f):[3]

$$z_d = d_f \cdot \left[\left[\frac{\mathrm{NA}^2 (n^2\text{-}1)}{1-\mathrm{NA}^2} + n^2 \right]^{1/2} - n \right] \quad (1)$$

As shown in Figure S9(b), the backscattered Raman light from the focus point p_1 is homogeneous in all directions. Then, the collection efficiency can be simply determined by the detection angle within which the light can pass through the confocal aperture.[4] Figure S9(c) shows the normalized intensity change of Raman peak centered at 1006 cm^{-1} with respect to different focus depth. It can be seen that the Raman peak intensity is significantly affected by focus depth. The intensity fluctuations along with the focal depth were also obvious due to the difficulties of precisely locating the focal point with a blurry vision when focused inside the fluid.

Table S1. Spectral interpretations of urea and pHEMA.

Urea	Assignments
530	δ(CN)
1006	v_{as}(CN)
1150	ρ_s(NH_2)

pHEMA	Assignments
899	*vs*(C-C)
966	ρ(CH3)
1028	*v* (C-C)
1088	ρ(CH_2)
1123	*v* (C=O)
1276	*w*(CH_2)
1455	δ(CH_3)

w–wagging, δ-scissoring, *v*-stretching, ρ-rocking, s-symmetric, as-asymmetric

Reference

1. L. Durlofsky, J. F. Brady, *Phys. Fluids*, 1987, **30**, 3329.
2. F. Fornasiero, D. Tang, A. Boushehri, J. Prausnitz and C. J. Radke, *J. Membr. Sci.*, 2008, **320**, 423.
3. N. J. Everall, *Appl. Spectrosc.*, 2000, **54**, 1515.
4. K. J. Baldwin and D. N. Batchelder, *Appl. Spectrosc.*, 2001, **55**, 517.